

Antibacterial and Antibiofilm Efficacy of a Synthetic Nitrofuranyl Pyranopyrimidinone Derivative against Methicillin-Resistant *Staphylococcus aureus*

Sepideh Soltani¹ , Nasrin Saberi Harooni² , Fatemeh Dehghani Tafti² , Morvarid Shafiei^{*} , Azar Tahghighi^{2*} 

¹Department of Bacteriology, Pasteur Institute of Iran, Tehran, Iran; ²Medicinal Chemistry Laboratory, Department of Clinical Research, Pasteur Institute of Iran, Tehran, Iran

ARTICLE INFO

Original Article

Keywords: Methicillin-resistant *Staphylococcus aureus*, pyranopyrimidinone, antibiofilm agents, confocal laser scanning microscopy

Received: 01 Dec. 2024

Received in revised form: 26 Feb. 2025

Accepted: 10 Mar. 2025

DOI: 10.61186/JoMMID.13.2.139

*Correspondence

Email: dr.shafiei80@gmail.com

atahghighi2009@gmail.com

Tel: +982164112231

© The Author(s)



ABSTRACT

Introduction: Methicillin-resistant *Staphylococcus aureus* (MRSA) is a major public health concern due to its multidrug resistance and robust biofilm formation, which contribute to persistent infections and treatment failures. Novel antibiofilm agents are urgently needed to combat drug-resistant pathogens. This study evaluated the antibacterial and antibiofilm efficacy of NFPPO, a novel nitrofuranyl pyranopyrimidinone derivative, against preformed 1-, 3-, and 5-day-old MRSA biofilms. **Methods:** NFPPO was synthesized via a tandem Knoevenagel-Michael cyclocondensation reaction. The minimum inhibitory concentration (MIC) of NFPPO was determined against four clinical MRSA isolates and the reference strain *S. aureus* ATCC 700699. Antibiofilm activity was assessed against preformed 1-, 3-, and 5-day-old MRSA biofilms using the crystal violet assay. Confocal laser scanning microscopy (CLSM) quantified structural and viability changes in preformed biofilms post-NFPPO treatment. **Results:** All tested MRSA isolates and *S. aureus* ATCC 700699 exhibited vancomycin resistance (classified as VRSA), whereas NFPPO showed potent antibacterial activity (MIC, 8–16 µg/mL). All isolates formed robust biofilms (OD₆₂₅ ≥ 3.0). Crystal violet assays and CLSM demonstrated significant NFPPO antibiofilm activity, reducing biofilm biomass and viability. **Conclusions:** NFPPO exhibited superior antibiofilm efficacy compared to vancomycin in eradicating *in vitro* preformed 1-, 3-, and 5-day-old MRSA biofilms. These findings position NFPPO as a promising candidate for further development to target biofilm-associated MRSA infections.

INTRODUCTION

Staphylococcus aureus is a predominant pathogen responsible for diverse infections, including endocarditis, pneumonia, septicemia, and infections of the bone, joints, skin, and soft tissues [1]. Of critical concern is MRSA, a global health priority due to its high morbidity, mortality, and substantial economic burden on healthcare systems [2]. MRSA has increasingly been detected beyond traditional healthcare-associated settings, with reports of colonization and infections in community-associated settings, such as sports facilities, restaurants, outpatient clinics, and community populations [3, 4]. Alarming, MRSA incidence rates have surged over the past decade, highlighting an urgent public health crisis [5].

The ability of staphylococci, particularly *S. aureus* and *Staphylococcus epidermidis*, to form biofilms is a well-established virulence factor that drives persistent and recalcitrant infections [6]. In MRSA strains, biofilm formation, coupled with their intrinsic multidrug-resistant phenotypes, significantly enhances resistance to antimicrobial agents and evasion of host immune responses [7]. Furthermore, biofilms facilitate horizontal gene transfer (HGT) mechanisms, such as conjugation and transformation, which promote the spread of antimicrobial resistance genes among bacterial populations [8].

The process of biofilm formation in *S. aureus* is widely acknowledged to proceed through four principal stages:

initial adhesion, aggregation, maturation, and eventual dispersion of bacterial cells [6]. During these stages, *S. aureus* utilizes diverse factors and regulatory mechanisms, particularly the expression of cell wall-anchored proteins (CWPs), alongside other surface components [9]. Following adhesion to surfaces, the attached bacterial cells initiate proliferation and aggregation when exposed to an adequate nutrient source [6]. During the aggregation stage, bacteria orchestrate biofilm formation by sensing environmental signals that activate intricate regulatory networks and intracellular signaling molecules. Simultaneously, bacteria continue to proliferate and progressively develop into a more resilient and intricate biofilm architecture, thereby enhancing their resistance to antibiotics and the host immune system [10]. During the maturation stage, the biofilm structure becomes highly structured, developing a dense, three-dimensional, and frequently mushroom-like architecture. Mature biofilms exhibit a wide array of specialized metabolic activities that confer increased resilience to adverse environmental factors and stress conditions [6].

Vancomycin has long been regarded as a cornerstone therapeutic agent for infections caused by MRSA. However, the widespread and frequently indiscriminate use of vancomycin has led to the emergence of MRSA strains with reduced susceptibility to this antibiotic. Moreover, *S. aureus* can develop vancomycin resistance (VRSA, MIC \geq 16 μ g/mL), primarily driven by the horizontal transfer of resistance genes, such as *vanA* and *vanB*, from vancomycin-resistant enterococci [11].

The rising prevalence of multidrug-resistant MRSA strains, driven by widespread inappropriate antibiotic use, has made effective treatment increasingly challenging [12]. Consequently, the development of innovative and effective therapeutic strategies to combat MRSA infections has become critically important. In particular, targeting the eradication of established biofilms represents a highly promising therapeutic approach, as it could significantly reduce morbidity and mortality associated with persistent MRSA infections, thereby addressing a major unmet medical need [13].

Pyrano [2, 3-d] pyrimidines, a prominent class of polycyclic compounds, have exhibited significant antimicrobial activity against a broad spectrum of bacterial species, particularly *S. aureus* [14-18]. In our previous work, we reported the synthesis of a series of pyrano[2,3-d]pyrimidinone carbonitrile derivatives via a one-pot synthetic approach using a nanocatalyst, minimizing solvent use and waste. This methodology provided several advantages, including operational simplicity, ease of purification, reduced waste generation, cost efficiency, and high product yields [19].

Notably, the synthetic nitrofurane derivative NFPPO exhibited broad-spectrum antibacterial activity against a diverse panel of bacterial strains, including antibiotic-susceptible laboratory strains and clinically relevant multidrug-resistant isolates [19]. In particular, NFPPO

demonstrated superior antibacterial efficacy against a prototype methicillin-resistant *Staphylococcus aureus* (MRSA) strain compared to levofloxacin, a fluoroquinolone reference agent. However, the antibiofilm efficacy of NFPPO against MRSA, especially its capacity, to disrupt mature biofilms-remains poorly characterized [19, 20]. To address this gap, the present study aimed to systematically evaluate and compare the antibacterial and antibiofilm activities of NFPPO against vancomycin, a last-line glycopeptide antibiotic used for MRSA infections. Additionally, CLSM was employed to visualize the three-dimensional architecture and viability of NFPPO-treated MRSA ATCC 700699 biofilms, providing mechanistic insights into its mode of action.

MATERIAL AND METHODS

Bacterial isolation and antibiotic resistance profiling. Sixteen clinical isolates were collected from diabetic wound infections in patients admitted to Loghman-Hakim Hospital, between November 2021 to January 2023. Identification of *S. aureus* was confirmed by routine microbiological assays, including Gram staining, catalase test, and coagulase test.

MRSA screening was performed using antimicrobial susceptibility testing (AST) via disk diffusion with oxacillin (1 μ g) and cefoxitin (30 μ g) disks, following CLSI M100 guidelines [21]. Genotypic confirmation of methicillin resistance was achieved by polymerase chain reaction (PCR) targeting the *mecA* gene, using specific primers [21].

The reference strain, *S. aureus* ATCC 700699, was procured from the microbial culture collection of the Pasteur Institute of Iran (Tehran, Iran). All confirmed MRSA isolates were cryopreserved in tryptic soy broth (TSB) supplemented with 20% glycerol at -20°C for long-term storage and subsequent analyses.

The antibiotic resistance profiles of the isolates were determined in accordance with the latest CLSI guidelines (2024). Antimicrobial susceptibility testing (AST) of *S. aureus* isolates was performed using the disk diffusion method on Mueller-Hinton agar medium (Merck, Germany). The following antimicrobial agents, representing five distinct classes, were evaluated: aminoglycosides (gentamicin), macrolides (erythromycin and azithromycin), tetracyclines (doxycycline), fluoroquinolones (ciprofloxacin and levofloxacin), and lincosamides (clindamycin). Multidrug resistance (MDR) was defined as non-susceptibility to at least one antimicrobial agent in three or more of the tested classes [21].

Synthesis of NFPPO. The target compound, NFPPO, was synthesized according to Figure 1 [19]. A mixture of 5-nitro-2-furaldehyde (1, 1 mmol), malononitrile (2, 1.2 mmol), and MWCNTs/Cu/Co/Ni catalyst (0.0024 g) in absolute ethanol (10 mL, 99.9% purity) was refluxed at 80°C for 15 minutes.

The reaction progress was monitored by thin-layer chromatography (TLC) to ensure complete consumption of the aldehyde. Subsequently, 1,3-dimethylbarbituric acid (3, 1 mmol) was added to the mixture, and the

reaction was maintained at 50–60°C until precipitation was complete. The resulting NFPPO precipitates were collected by filtration, washed with cold ethanol (15 mL, 3 × 5 mL), and dried at ambient temperature (25°C) to yield the pure target compound in 70% yield.

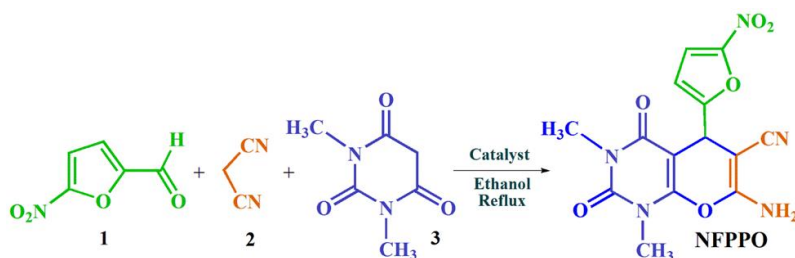


Fig. 1. Synthesis of NFPPO derivatives via a tandem Knoevenagel-Michael cyclocondensation reaction catalyzed by a nanocatalyst (MWCNTs/Cu/Co/Ni) in ethanol.

Determination of MIC and minimum bactericidal concentration (MBC) of vancomycin and NFPPO. The MIC was determined by the broth microdilution method as described. Antibiotic stock solutions were prepared and diluted according to Clinical and Laboratory Standards Institute (CLSI 2024) protocols. Purified powder of vancomycin was obtained from Sigma-Aldrich, USA. NFPPO and vancomycin were dissolved in DMSO and sterile distilled water, respectively. Concentration ranges for vancomycin and NFPPO were 0.5–512 µg/mL, following CLSI M100 guidelines. Microtiter plates were inoculated with bacteria with a turbidity of 1.6×10^8 CFU/mL and incubated aerobically at 37°C for 24 h. The MBC was determined after broth microdilution by sub-culturing a sample from wells, yielding negative microbial growth after incubation on the surface of non-selective agar plates. After 24 h of incubation, MBC was defined as the lowest concentration that killed 99.9% of the final inoculum. MIC and MBC values were determined at least in duplicate and repeated to confirm activity.

Biofilm formation assay. The biofilm-forming ability of MRSA strains was assessed using a modified protocol based on Shafiei *et al.* (2014). Briefly, a 96-well flat-bottom polystyrene microtiter plate (Sigma-Aldrich, St. Louis, MO, USA) was employed for biofilm quantification. Overnight cultures of each strain were grown in tryptic soy broth supplemented with 0.2% glucose (Merck, Germany) at 37°C for 24 hours. Bacterial suspensions were prepared in tryptic soy broth supplemented with 0.2% glucose and adjusted to a 0.5 McFarland standard turbidity (approximately 1.5×10^8 CFU/mL, OD 0.08–0.1 at 625 nm) using a spectrophotometer. Suspensions were diluted 1:100 in fresh medium, and 200 µL was aliquoted into each well of the microtiter plate. Plates were incubated statically at 37°C for 24 hours.

After incubation, the planktonic cells and medium were aspirated, and wells were gently washed three times with sterile phosphate-buffered saline (PBS) to remove non-

adherent cells. Adherent biofilms were fixed with absolute methanol for 10 minutes, air-dried, and stained with 1% (w/v) crystal violet for 15 minutes at room temperature. Excess stain was removed by rinsing the plates three times with sterile distilled water. Bound dye was solubilized using 200 µL of 33% (v/v) glacial acetic acid, and the OD of each well was measured at 625 nm using a microplate reader. Sterile medium and bacterial suspensions served as negative and positive controls, respectively.

Biofilm formation was categorized based on OD595 values: strongly adherent (OD ≥ 3.0), moderately adherent (OD 1.5–2.0), weakly adherent (OD 0.5–1.0), or non-adherent (OD \leq negative control OD575). OD < 0.5 was considered negative [22]. All assays were performed in duplicate to ensure reproducibility.

Biofilm eradication assay. The effect of vancomycin and NFPPO on pre-formed biofilms was evaluated using 96-well microtiter plates. Bacterial suspensions were prepared in tryptic soy broth supplemented with 0.2% glucose to a final concentration of 1×10^6 CFU/mL, and 100 µL of the suspension was added to each well. After 1, 3, and 5 days of incubation at 37°C, the plates were treated with serial dilutions of vancomycin and NFPPO at concentrations corresponding to 1:8 MIC, 1:4 MIC, 1:2 MIC, 1× MIC, 2× MIC, 4× MIC, and 8× MIC. The plates were then incubated for an additional 24 hours at 37°C.

After incubation, the medium was gently aspirated, and the biofilms were fixed with 100% methanol for 15 minutes. The methanol was then removed, and the plates were air-dried. The wells were stained with 1% (w/v) crystal violet for 30 minutes, after which the stain was removed, and the wells were rinsed three times with distilled water to remove excess dye. The plates were air-dried again, and the bound crystal violet was solubilized using 95% ethanol. The wells were visually inspected for turbidity, and the optical density was measured using a microplate reader [22].

The minimum biofilm eradication concentration (MBEC) was defined as the lowest concentration of vancomycin or NFPPO that resulted in a $\geq 99.9\%$ reduction in viable biofilm cells, with no observable regrowth after 24 h of exposure. All experiments were performed in duplicate to ensure reproducibility.

Analysis of biofilms by Confocal Laser Scanning Microscopy (CLSM). CLSM was employed to evaluate the effect of NFPPO on pre-formed biofilms of MRSA ATCC 700699. Briefly, six-well microtiter plates containing sterile glass coverslips were incubated with 5 mL of TSB supplemented with 2% glucose at 37°C for 24 hours. Each well was inoculated with 1 mL of mid-exponential-phase bacterial cultures (adjusted to $\sim 1 \times 10^6$ CFU/mL). After 24 hours of incubation, NFPPO was added to the wells at its MBEC and incubated for an additional 24 hours at 37°C.

Following treatment, the coverslips were carefully removed, gently rinsed with sterile PBS, and stained with 15 μ L of propidium iodide (PI; 1 mg/mL, Sigma-Aldrich, USA) for 15 minutes at room temperature in the dark to label dead bacterial cells (red fluorescence). After washing with PBS, the biofilms were stained with 50 μ g/mL fluorescein isothiocyanate (FITC; Sigma-Aldrich, USA) for 15 minutes at room temperature to visualize the glycocalyx matrix (green fluorescence). Although their standard excitation/emission maxima are $\sim 495/519$ nm (FITC) and $\sim 535/617$ nm (PI), images were acquired using confocal microscopy settings optimized to 495/525 nm (FITC) and 520/620 nm (PI), according to the instrument's filter specifications.

Confocal images were acquired using a Leica TCS SP8 CLSM system (Leica Microsystems, Germany). Biofilm parameters (biomass, thickness, surface coverage) were quantitatively analyzed using COMSTAT 2.1 software.

Statistical analysis. Statistical analyses were performed using Microsoft Excel 2013 (Microsoft Corp.,

USA) for descriptive statistics and SPSS v17.0 (IBM Corp., USA) for t-tests and ANOVA. A paired t-test was used to compare the effects of vancomycin and NFPPO on biofilm eradication for each time point (1, 3, and 5 days), while a one-way ANOVA was performed to assess differences across time points within each treatment. A P -value < 0.05 was deemed statistically significant. Quantitative three-dimensional biofilm structural parameters, including biomass, thickness, and surface coverage, were analyzed using COMSTAT 2.1 software.

Ethical considerations. This study was conducted in accordance with the ethical guidelines and received formal approval from the Research Ethics Committee of the Pasteur Institute of Iran (Approval Code: IR.PIL.REC.1400.086).

RESULTS

Bacterial isolation and antibiotic resistance profile.

In this study, a total of 16 *S. aureus* strains, comprising 4 (25%) MRSA and 12 (75%) methicillin-susceptible *S. aureus* (MSSA), were isolated. The MRSA isolates (MRSA IM15, MRSA IM16, MRSA IM17, MRSA IM18) as well as MRSA ATCC 700699 were used for further analysis. AST results revealed that all MRSA isolates exhibited a multidrug-resistant (MDR) phenotype.

MICs and MBCs of vancomycin and NFPPO. The MIC and MBC values of vancomycin and NFPPO against four MRSA isolates and the reference MRSA strain, *S. aureus* ATCC 700699, are summarized in Table 1. The MIC results revealed that all isolates exhibited intermediate to high-level resistance to vancomycin, as per the CLSI guidelines. Based on these findings, all MRSA isolates were classified as VRSA. Notably, the MIC and MBC values of NFPPO were identical for each MRSA isolate, indicating bactericidal activity.

Table 1. MICs and MBCs of vancomycin and NFPPO against four clinical MRSA isolates and one reference MRSA strain

Strains	Vancomycin (μ g/mL)		NFPPO (μ g/mL)	
	MIC	MBC	MIC	MBC
MRSA ATCC 700699	R	-	16	16
MRSA IM15	R	-	16	16
MRSA IM16	R	-	16	16
MRSA IM17	R	-	8	8
MRSA IM18	R	-	8	8

R: Resistant

Biofilm formation ability. Quantitative biofilm assays revealed that all clinical MRSA isolates exhibited robust biofilm-forming capacity, with OD₅₉₅ values ≥ 3.0 , indicating strong biofilm production.

Biofilm eradication activity of vancomycin and NFPPO. The MBECs of vancomycin and NFPPO against 1-, 3-, and 5-day-old biofilms are summarized in Table 2. Notably, NFPPO eradicated all MRSA isolates, with MBEC values ranging from 7.8 to 62.5 μ g/mL, whereas

vancomycin exhibited significantly higher MBECs (128–512 μ g/mL). Strikingly, while vancomycin required high concentrations to disrupt biofilms of all ages (1-, 3-, and 5-day-old), NFPPO demonstrated superior efficacy, achieving a $\geq 99.9\%$ reduction in viable biofilm cells at substantially lower concentrations (Figure 2). NFPPO was significantly more effective than vancomycin in eliminating biofilms of clinical MRSA isolates ($P < 0.01$, paired t-test, for all time points and strains).

Table 2. MBEC of vancomycin and NFPPO against 1-, 3-, and 5-day-old biofilms

Strain	Vancomycin (µg/mL)			NFPPO (µg/mL)		
	1-day	3-day	5-day	1-day	3-day	5-day
MRSA ATCC 700699	128	128	256	7.8	15.6	31.2
MRSA IM15	128	256	512	31.2	31.2	62.5
MRSA IM16	256	256	512	15.6	31.2	31.2
MRSA IM17	128	512	512	31.2	62.5	62.5
MRSA IM18	256	256	512	31.2	31.2	62.5

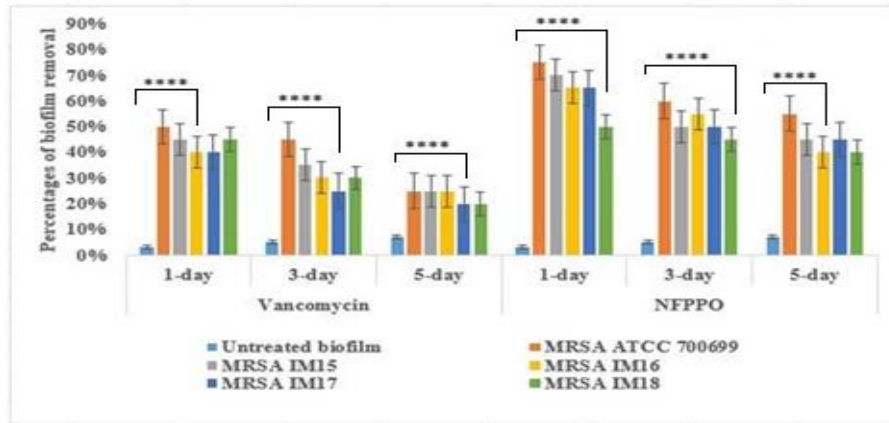


Fig. 2. Biofilm reduction over time with vancomycin and NFPPO. Bar plot showing the percentages of biofilm removal in MRSA strains treated with vancomycin and NFPPO over 1, 3, and 5 days. Statistical significance was assessed using t-test and one-way ANOVA. Asterisks (****) shows P -value < 0.0001 . Error bars represent standard deviations of the mean from replicate experiments.

Observation of biofilms by CLSM. Representative CLSM images of NFPPO-treated and untreated biofilms are shown in Figure 3. The proportion of the adherence area was used as an indicator of biofilm eradication efficiency. In the untreated control group, 95% of biofilm cells were viable (based on PI/FITC staining), whereas

following NFPPO treatment, viable cells were reduced to 45%. A significant reduction in biofilm biomass was observed in the NFPPO-treated group compared to the untreated control ($P < 0.001$, paired t-test; Table 3). Collectively, these findings demonstrate that NFPPO exhibits considerable antibiofilm activity against preformed MRSA biofilms.

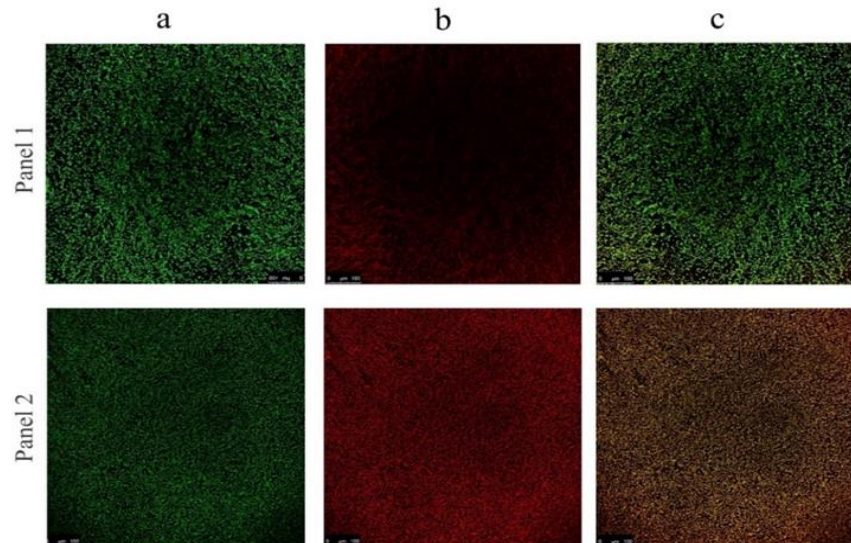


Fig. 3. CLSM Micrographs of *S. aureus* ATCC 700699 Biofilms. CLSM images illustrating the antibiofilm activity of NFPPO against MRSA biofilms. Panel 1 (a–c) represents untreated (native) biofilms, while Panel 2 (a–c) depicts NFPPO-treated biofilms

Table 3. Quantitative biofilm analysis using COMSTAT software

Parameter	Control (untreated biofilm)	NFPPO-treated group	P-value
Surface area	74,450	52015	-
Surface-to-biovolume ratio	1.462	0.645	5.8×10^{-8}
Biomass	0.7376	0.450	1.47×10^{-6}

DISCUSSION

MRSA is a leading pathogen responsible for chronic infections, largely due to its robust biofilm-forming capacity [23]. The emergence of multidrug resistance in MRSA, coupled with the paucity of novel antimicrobial agents effective against this pathogen, has raised significant global public health concerns. This challenge poses a critical threat to healthcare systems worldwide, with projections indicating substantial economic burdens in the coming decades [24]. In response, diverse therapeutic strategies—including bacteriophages, phytochemicals, antimicrobial peptides (AMPs), nanoparticles, and repurposed drugs—are being explored as complementary or alternative antibiofilm agents [25, 26]. In this study, we focused on the synthetic nitrofuranyl pyranopyrimidinone derivative NFPPO, which demonstrated promising antibacterial activity against drug-sensitive and multidrug-resistant *S. aureus* strains in prior work [19]. Here, we evaluated the efficacy of NFPPO against preformed MRSA biofilms, using vancomycin as a comparator. Our findings reveal that NFPPO exhibits superior antibiofilm activity compared to vancomycin, significantly reducing biofilm biomass and viability at lower concentrations.

The synthetic compound NFPPO features a 5-nitrofuranyl moiety integrated into an amino pyrano[2,3-d]pyrimidinone carbonitrile framework, a structural motif shared by established antibacterial nitrofuranyl drugs (NFs) such as nitrofurazone, nifuroxazide, nitrofurantoin, and ranbezolid. Nitrofurazone, a potent bactericidal agent, has demonstrated significant efficacy against *S. aureus* [27]. Similarly, nifuroxazide—a broad-spectrum intestinal antibacterial agent—exhibits both bactericidal and bacteriostatic activity, particularly against MRSA, mirroring the pharmacological profile of nitrofurantoin [27].

The enzymatic reduction of nitrofurans (NFs) by bacterial nitroreductases (type I or II) generates highly reactive electrophilic intermediates, which inhibit bacterial enzymes and ultimately lead to bacterial cell death [13, 27, 28]. These nitroreductases, which are abundantly expressed in bacteria but absent in humans, catalyze the NADPH-dependent reduction of NFs [29]. The nitro group in NFs enhances their therapeutic activity, while electron delocalization within the nitrofuranyl ring contributes to their chemical stability. Moreover, the strong electron-withdrawing nature of the NO₂ group induces electron deficiency in the furan ring, facilitating the reduction of the nitrofuranyl ring and generating highly reactive intermediates [30].

Numerous studies have highlighted the critical role of aryl/heteroaryl scaffolds with nitro substitutions in potentiating antibacterial activity, particularly against *S. aureus* and MRSA biofilms [31, 32]. Among these, the nitrofuranyl ring appears to be central to the potent antibiofilm activity of NFs. Type I nitroreductases catalyze the reduction of the nitro group into reactive nitroso and hydroxylamine derivatives, which can further convert into nitric oxide—a known dispersant of MRSA biofilms [33].

For instance, Kavaliauskas *et al.* (2020) [31] demonstrated that KTU-286, a compound containing a 5-nitro-thiophene moiety, exhibits significant antibiofilm activity against multidrug-resistant *S. aureus*. Similarly, Kamal *et al.* (2013) [32] reported that 1,2,3-triazole-nitrofuranyl hybrids display potent anti-MRSA activity and notable antibiofilm efficacy against *S. aureus* MLS-16 MTCC 2940. Based on these findings, we propose that NFPPO, which contains a 5-nitrofuranyl moiety, likely shares a similar mechanism of action with the NFs described above.

In contrast to vancomycin, which required high concentrations to eradicate biofilms, NFPPO demonstrated potent antibiofilm activity against preformed MRSA biofilms at significantly lower concentrations. Quantitative analysis via CLSM and 96-well microtiter plate assays revealed significant biofilm reduction by NFPPO. The enhanced antimicrobial activity of NFPPO is likely attributable to its molecular architecture, featuring a heterocyclic fused amino pyrano[2,3-d]pyrimidinone carbonitrile scaffold conjugated with a nitro group, a strong electron-withdrawing moiety, potentially enhancing target binding and reactive intermediate generation.

The emergence of drug-resistant *S. aureus* and its ability to form biofilms pose significant challenges in the treatment of infections, contributing to elevated morbidity and mortality rates worldwide. In light of this, there is an urgent need for novel therapeutic strategies to address MRSA infections and their associated biofilms in clinical settings. In this study, NFPPO demonstrated potent antibacterial and antibiofilm activity against four clinically relevant MRSA isolates, outperforming vancomycin. Additionally, the straightforward synthesis and high yield of NFPPO production highlight its potential for further development as an antibacterial agent. However, to fully realize its therapeutic potential, further investigations are required, including *in vivo* studies, pharmacokinetic profiling, and formulation optimization to minimize the effective dose. These steps are essential to potentially replace commercially available

antibiotics that have diminished efficacy due to widespread drug tolerance and resistance. In conclusion, NFPPO shows promise as a potential antibacterial and antibiofilm agent for combating planktonic and biofilm-associated MRSA infections, pending further *in vivo* and clinical validation. Nevertheless, *in vivo* studies, pharmacokinetic analyses, and clinical trials are warranted to elucidate its therapeutic efficacy, safety profile, and clinical applicability.

CONFLICTS OF INTEREST

The authors declare that there are no conflicts of interest associated with this manuscript.

ACKNOWLEDGEMENT

The authors thank the Bacteriology and Medicinal Chemistry Departments at the Pasteur Institute of Iran for providing essential equipment and facilities. Their contributions were instrumental in the successful execution of this study.

AUTHORS' CONTRIBUTIONS

SS: Performed biological tests and drafted the initial version of the manuscript. NSH and FDT: Contributed to the synthesis of NFPPO and assisted in the development of some methodologies. MS: Designed the biological tests, analyzed the results, and revised the manuscript. AT: Conceived and designed the project, interpreted the data, and critically revised the manuscript. All authors reviewed and approved the final manuscript.

FUNDING

This study was conducted without any external financial support.

REFERENCES

1. Linz MS, Mattappallil A, D'Angelo DM. Clinical impact of *Staphylococcus aureus* skin and soft tissue infections. *Antibiotics*. 2023; 12 (3): 557.
2. Sergelidis D, Angelidis AS. Methicillin-resistant *Staphylococcus aureus*: a controversial food-borne pathogen. *Lett Appl Microbiol*. 2017; 64 (6): 409-18.
3. Wakabayashi Y, Takemoto K, Iwasaki S, Yajima T, Kido A, Yamauchi A, et al. Isolation and characterization of *Staphylococcus argenteus* strains from retail foods and slaughterhouses in Japan. *Int J Food Microbiol*. 2022; 363: 109503.
4. Lin JL, Peng Y, Ou QT, Lin DX, Li Y, Ye XH, et al. A molecular epidemiological study of methicillin-resistant *Staphylococci* environmental contamination in railway stations and coach stations in Guangzhou of China. *Lett Appl Microbiol*. 2017; 64 (2): 131-7.
5. Silva V, Almeida F, Carvalho JA, Castro AP, Ferreira E, Manageiro V, et al. Emergence of community-acquired methicillin-resistant *Staphylococcus aureus* EMRSA-15 clone as the predominant cause of diabetic foot ulcer infections in Portugal. *Eur J Clin Microbiol Infect Dis*. 2020; 39 (1): 179-6.
6. Peng Q, Tang X, Dong W, Sun N, Yuan W. A review of biofilm formation of *Staphylococcus aureus* and its regulation mechanism. *antibiotics (Basel)*. 2022; 12 (1): 12.
7. Ning Y, Wang X, Chen P, Liu S, Hu J, Xiao R. Targeted inhibition of methicillin-resistant *Staphylococcus aureus* biofilm formation by a graphene oxide-loaded aptamer/berberine bifunctional complex. *Drug Deliv*. 2022; 29 (1): 1675-83.
8. Silva V, Almeida L, Gaio V, Cerca N, Manageiro V, Caniça M. Biofilm formation of multidrug-resistant MRSA strains isolated from different types of human infections. *Pathogens*. 2021; 10 (8): 970.
9. Schilcher K, Horswill AR. Staphylococcal biofilm development: structure, regulation, and treatment strategies. *Microbiol Mol Biol Rev*. 2020; 84 (3): e00026-19.
10. Idrees M, Sawant SH, Karodia N, Rahman A. *Staphylococcus aureus* biofilm: morphology, genetics, pathogenesis and treatment strategies. *Int J Environ Res Public Health*. 2021; 18 (14): 7602.
11. Luna CM, Rodríguez-Noriega E, Bavestrello L, Gotuzzo E. Treatment of methicillin-resistant *Staphylococcus aureus* in Latin America. *Braz J Infect Dis*. 2010; 14 Suppl 2: S119-27.
12. Nazli A, Tao W, You H, He X, He Y. Treatment of MRSA infection: where are we? *Curr Med Chem*. 2024; 31 (28): 4425-60.
13. Verderosa AD, Totsika M, Fairfull-Smith KE. Bacterial biofilm eradication agents: a current review. *Front Chem*. 2019; 7: 824.
14. Abd El-Sattar NEA, El-Adl K, El-Hashash MA, Salama SA, Elhady MM. Design, synthesis, molecular docking and *in silico* ADMET profile of pyrano[2,3-d]pyrimidine derivatives as antimicrobial and anticancer agents. *Bioorg Chem*. 2021; 115: 105186.
15. Ziarani GM, Nasab NH, Rahimifard M, Soorki AA. One-pot synthesis of pyrido[2,3-d]pyrimidine derivatives using sulfonic acid functionalized SBA-15 and the study on their antimicrobial activities. *J Saudi Chem Soc*. 2015; 19 (6): 676-81.
16. Yalagala K, Maddila S, Rana S, Maddila SN, Kalva S, Skelton AA. Synthesis, antimicrobial activity and molecular docking studies of pyrano[2,3-d]pyrimidine formimidate derivatives. *Res Chem Intermed*. 2016; 42 (4): 3763-74.
17. Aremu OS, Singh P, Singh M, Mocktar C, Koorbanally NA. Synthesis of chloro, fluoro, and nitro derivatives of 7-amino-5-aryl-6-cyano-5H-pyrano pyrimidin-2,4-diones using organic catalysts and their antimicrobial and anticancer activities. *J Heterocycl Chem*. 2019; 56 (11): 3008-16.
18. Aremu OS, Gopaul K, Kadam P, Mocktar C, Singh P, Koorbanally NA. Synthesis, characterization, anticancer and antibacterial activity of some novel pyrano[2,3-d]pyrimidinone carbonitrile derivatives. *Anticancer Agents Med Chem*. 2017; 17 (5): 719-25.
19. Saberi Harooni N, Dehghani Tafti F, Moghaddam N, Naeimi H, Azerang P, Tahghighi A. Antibacterial efficacy of

Soltani et al.

- pyranopyrimidinone derivatives synthesized using a facile one-pot reaction. *Re Chem Intermed*. 2024; 50 (9): 4533-50.
20. Zafari M, Adibi M, Chiani M, Bolourchi N, Barzi SM, Shams Nosrati MS, et al. Effects of cefazolin-containing niosome nanoparticles against methicillin-resistant *Staphylococcus aureus* biofilm formed on chronic wounds. *Biomed Mater*. 2021; 16 (3): 035001.
 21. Clinical and Laboratory Standards Institute. Performance Standards for Antimicrobial Susceptibility Testing. 34th ed. CLSI supplement M100. Wayne, PA: Clinical and Laboratory Standards Institute; 2024.
 22. Stepanović S, Vuković D, Hola V, Di Bonaventura G, Djukić S, Cirković I, et al. Quantification of biofilm in microtiter plates: overview of testing conditions and practical recommendations for assessment of biofilm production by staphylococci. *APMIS*. 2007; 115 (8): 891–9.
 23. Kaushik A, Kest H, Sood M, Steussy BW, Thieman C, Gupta S. Biofilm producing methicillin-resistant *Staphylococcus aureus* (MRSA) infections in humans: clinical implications and management. *Pathogens*. 2024; 13 (1): 76.
 24. Bremner JB. An update review of approaches to multiple action-based antibacterials. *Antibiotics (Basel)*. 2023; 12 (5): 865.
 25. Iaconis A, De Plano LM, Caccamo A, Franco D, Conoci S. Anti-biofilm strategies: a focused review on innovative approaches. *Microorganisms*. 2024; 12 (4): 639.
 26. Mohamad F, Alzahrani RR, Alsaadi A, Alrfai BM, Yassin AEB, Alkhulaifi MM. An explorative review on advanced approaches to overcome bacterial resistance by curbing bacterial biofilm formation. *Infect Drug Resist*. 2023; 16: 19-49.
 27. Zuma NH, Aucamp J, N'Da DD. An update on derivatisation and repurposing of clinical nitrofurans drugs. *Eur J Pharm Sci*. 2019; 140: 105092.
 28. Pala L, Sirec T, Spitz U. Modified enzyme substrates for the detection of bacteria: a review. *Molecules*. 2020; 25 (16): 3690.
 29. Roldán MD, Pérez-Reinado E, Castillo F, Moreno-Vivián C. Reduction of polynitroaromatic compounds: the bacterial nitroreductases. *FEMS Microbiol Rev*. 2008; 32 (3): 474-500.
 30. Chain EPoCitF. Scientific opinion on nitrofurans and their metabolites in food. *EFSA J*. 2015; 13 (6): 4140.
 31. Kavaliauskas P, Grybaite B, Mickevicius V, Petraitiene R, Grigaleviciute R, Planciuniene R, et al. Synthesis, ADMET properties, and *in vitro* antimicrobial and antibiofilm activity of 5-Nitro-2-thiophenecarbaldehyde N-((E)-(5-Nitrothienyl)methylidene)hydrazone (KTU-286) against *Staphylococcus aureus* with defined resistance mechanisms. *Antibiotics (Basel)*. 2020; 9 (9): 612.
 32. Kamal A, Hussaini SMA, Faazil S, Poornachandra Y, Reddy GN, Kumar CG, et al. Anti-tubercular agents. Part 8: synthesis, antibacterial and antitubercular activity of 5-nitrofurans based 1,2,3-triazoles. *Bioorg Med Chem Lett*. 2013; 23 (24): 6842-6.
 33. Ndukwe ARN, Qin J, Wiedbrauk S, Boase NRB, Fairfull-Smith KE, Totsika M. *In vitro* activities of oxazolidinone antibiotics alone and in combination with C-TEMPO against methicillin-resistant *Staphylococcus aureus* biofilms. *Antibiotics (Basel)*. 2023; 12 (12): 1706.

Cite this article:

Soltani S, Saberi Harooni N, Dehghani Tafti F, Shafiei M, Tahghighi A. Antibacterial and Antibiofilm Efficacy of a Synthetic Nitrofuranyl Pyranopyrimidinone Derivative against Methicillin-Resistant *Staphylococcus aureus*. *J Med Microbiol Infect Dis*, 2025; 13 (2): 139-146. DOI: 10.61186/JoMMID.13.2.139.